symmetry

Article

Numerical Analysis of Time-Fractional Porous Media and Heat Transfer Equations Using a Semi-Analytical Approach

Muhammad Nadeem [1,*], Asad Islam [2], Shazia Karim [3], Sorin Mureşan [4] and Loredana Florentina Iambor [4,*]

[1] School of Mathematics and Statistics, Qujing Normal University, Qujing 655011, China
[2] Department of Mechanical and Aerospace Engineering, Air University, Islamabad 44000, Pakistan; asad.islam@mail.au.edu.pk
[3] Department of Basic Sciences, UET Lahore, FSD Campus, Faisalabad 54800, Pakistan; shazia.karim@uet.edu.pk
[4] Department of Mathematics and Computer Science, University of Oradea, 1 University Street, 410087 Oradea, Romania; smuresan@uoradea.ro
[*] Correspondence: nadeem@mail.qjnu.edu.cn (M.N.); iambor.loredana@uoradea.ro (L.F.I.)

Abstract: In nature, symmetry is all around us. The symmetry framework represents integer partial differential equations and their fractional order in the sense of Caputo derivatives. This article suggests a semi-analytical approach based on Aboodh transform ($\mathbb{A}$T) and the homotopy perturbation scheme (HPS) for achieving the approximate solution of time-fractional porous media and heat transfer equations. The $\mathbb{A}$T converts the fractional problems into simple ones and obtains the recurrence relation without any discretization or assumption. This nonlinear recurrence relation can be decomposed via the use of the HPS to obtain the iterations in terms of series solutions. The initial conditions play an important role in determining the successive iterations and yields towards the exact solution. We provide some numerical applications to analyze the accuracy of this proposed scheme and show that the performance of our scheme has strong agreement with the exact results.

Keywords: Aboodh transform; homotopy perturbation scheme; porous media and heat transfer equations; convergence analysis

check for updates

Citation: Nadeem, M.; Islam, A.; Karim, S.; Mureşan, S.; Iambor, L.F. Numerical Analysis of Time-Fractional Porous Media and Heat Transfer Equations Using a Semi-Analytical Approach. *Symmetry* **2023**, *15*, 1374. https://doi.org/10.3390/sym15071374

Academic Editor: Mariano Torrisi

Received: 15 June 2023
Revised: 4 July 2023
Accepted: 5 July 2023
Published: 6 July 2023

1. Introduction

In recent years, numerous researchers have investigated the study of fluid flow over various symmetries and their related properties in a wide range of applications in science and engineering. This symmetry analysis is significant, from both a theoretical and practical angle of study. In particular phenomena, various researchers and academics have constructed fluid flow over a symmetry idea and demonstrated the heat transfer model to obtain their efficient solutions [1,2]. A change that makes the differential equation compatible is considered a symmetry differential problem. In the presence of such symmetries, these types of differential problems might be solvable. Lie point symmetries are used to build the optimal system of one-dimensional Lie subalgebra [3]. In other words, symmetries can be evaluated via the results of an associated formulation of some differential problems [4,5]. These equations can occasionally be solved more quickly than the original differential equations. These equations have drawn a lot of attention due to their outstanding simulation over traditional integer-order differential equations for a variety of physical and biological phenomena. They are often used to explain the viscous materials, system of control, and signal analysis in a variety of fields, including physics, engineering, biology, economics, and much more [6–9].

Numerous scientists have provided various numerical and analytical schemes for deriving the solution of ordinary and fractional differential problems in science and engineering fields [10,11]. Ali et al. [12] obtained the solitary wave solution for a fractional-order general equal-width equation via a semi-analytical technique. Khalid et al. [13] considered the separation of a variable scheme to handle the stefan problems in the cylindrical form under the eigen conditions. Momani and Odibat [14] implemented two analytical schemes to obtain the approximate results of linear PDEs in the Caputo-sense fractional derivatives. Cakmak and Alkan [15] studied the nonlinear Pantograph problems and provided approximate solutions via the Fibonacci collocation approach. Nuruddeen and Nass [16] utilized the Kudryashov method to obtain the solitary solution of the GEW-burgers problems. Iqbal et al. [17] obtained the numerical solution for the fractional-order Kersten–Krasil'shchik coupled KdV-mKdV system using the Atangana–Baleanu derivative. Mansal and Sene [18] obtained the analysis of a fractional model in the context of time-fractional order. Fang et al. [19] presented a novel scheme for the solution of Klein–Gordon and Sine–Gordon problems. Shah et al. [20] utilized the Laplace decomposition transform method to compute series-type solutions under fuzzy fractional PDEs. Nadeem and Li [21] proposed a significant scheme based on the Mohand transform and the HPS to derive the solution of fourth-order parabolic PDEs with fractional derivatives. Merdan [22] used the fractional variational iteration method for finding the approximate analytical solutions of the nonlinear fractional Klein–Gordon equation with the Riemann–Liouville sense. Arasteh et al. [23] emphasized the desire to investigate the partially embedded porous medium in a channel due to its numerous application uses in heat transfer and fluid flows. Barnoon et al. [24] investigated the heat transfer and non-Newtonian nanofluid flow in a porous enclosure with two cylinders inserted in the cavity with and without the effect of thermal radiation. A recent study on porous media and heat transfer equations can be found in [25–28]. The heat transfer and fluid flow of a channel are mostly unexplored. This is true even though numerous research has addressed the demand to explore the porous media partially embedded in a channel due to its numerous technical uses. To address this theory and difference, we carried out a study with a three-layered porous medium (occupying 60% of a heat sink) across Reynolds numbers ranging from 50 to 150 and water base fluid.

The Aboodh homotopy perturbation transform scheme ($\mathbb{A}$HPTS) is a committing strategy to derive the solution of fractional PDEs. This strategy has various advantages over traditional numerical schemes for the solution of PDEs of time-fractional order. Firstly, the $\mathbb{A}$HPTS is a semi-analytical approach where the analytical and numerical schemes are combined to obtain the results of the fractional differential problems. Moreover, this allows more precise results in the comparison of purely numerical schemes and also minimizes the heavy computational work compared to the other analytical techniques. Secondly, the $\mathbb{A}$HPTS has the advantage of overcoming the fractional PDEs, which makes it a fascinating approach for the outcome of broad challenges. Finally, the $\mathbb{A}$HPTS is a computationally efficient approach for solving fractional PDEs since it is simple to develop and can be promptly parallelized. We start this paper as follows: We present some preliminaries and concept of the $\mathbb{A}$T in Section 2. The development of $\mathbb{A}$HPTS and its convergence analysis are provided in Sections 3 and 4. In Section 5, we tested this semi-analytical scheme on the time-fractional porous media and heat transfer equations and showed that the proposed strategy is valid. In the end, we conclude the results in Section 6.

2. Preliminaries of $\mathbb{A}$T

This segment describes some preliminaries and the concept of $\mathbb{A}$T, which will be further use to construct the idea of a semi-analytical approach.

Definition 1. *The Caputo definition of order α is described as [29]:*

$$D_t^{\alpha}\vartheta(t) = \frac{1}{\Gamma(k-\alpha)}\int_0^t (t-\phi)^{k-\alpha-1}\vartheta^{(k)}(x,\phi)d\phi, \qquad k-1<\alpha\leq k. \tag{1}$$

Definition 2. *The $\mathbb{A}T$ for a function of $\vartheta(t)$ is defined as [29]:*

$$\mathbb{A}[\vartheta(t)] = R(w) = \frac{1}{w}\int_0^\infty e^{-wt}\vartheta(t)dt, \quad t \geq 0, \quad k_1 \leq w \leq k_2. \tag{2}$$

where $\mathbb{A}$ denotes the sign of $\mathbb{A}T$, and k_1 and k_2 are parameters, whereas w is the transformation element of the variable time function t. Conversely, $R(w)$ is the $\mathbb{A}T$ of $\vartheta(t)$; then,

$$\mathbb{A}^{-1}[R(w)] = \vartheta(t), \quad \mathbb{A}^{-1} \text{ is known as the inverse } \mathbb{A}\text{T}.$$

Proposition 1. *The linear property of $\mathbb{A}T$ is defined as [30].*
Let $\mathbb{A}\{\vartheta_1(t)\} = R_1(w)$ and $\mathbb{A}\{\vartheta_2(t)\} = R_2(w)$; then,

$$\begin{aligned} &\mathbb{A}\{a\vartheta_1(t) + b\vartheta_2(t)\} = a\mathbb{A}\{\vartheta_1(t)\} + b\mathbb{A}\{\vartheta_2(t)\}, \\ \Rightarrow\quad &\mathbb{A}\{a\vartheta_1(t) + b\vartheta_2(t)\} = aR_1(w) + bR_2(w). \end{aligned} \tag{3}$$

Proposition 2. *The differential properties are defined as [29,30].*
If $\mathbb{A}\{\vartheta(t)\} = R(w)$, then

$$\begin{aligned} (\mathbf{i}) \qquad & \mathbb{A}\{\vartheta'(x,t)\} = wR(x,w) - \frac{\vartheta(0)}{w}, \\ t(\mathbf{ii}) \qquad & \mathbb{A}\{\vartheta''(x,t)\} = w^2R(x,w) - \vartheta(0) - \frac{\vartheta'(0)}{w}, \\ (\mathbf{iii}) \qquad & \mathbb{A}\{\vartheta^m(x,t)\} = w^mR(x,w) - \frac{\vartheta(0)}{w^{2-m}} - \frac{\vartheta'(0)}{w^{3-m}} - \cdots - \frac{\vartheta^{m-1}(0)}{w}. \end{aligned} \tag{4}$$

Proposition 3. *The fractional differential property is defined as [30].*
If $\mathbb{A}\{\vartheta(t)\} = R(w)$, then

$$\mathbb{A}\{D_t^\alpha\vartheta(x,t)\} = w^\alpha R(x,w) - \Sigma_{k=0}^{r-1}\frac{\vartheta^{(k)}(x,0)}{w^{k-\alpha+2}}. \tag{5}$$

3. Formulation of $\mathbb{A}$HPTS

This segment demonstrates the construction of $\mathbb{A}$HPTS based on the combined form of the Aboodh transform and the homotopy perturbation scheme. The scheme does not require any theory of assumption and restriction of any elements. We start the formulation of this scheme by considering the following fractional differential problems as

$$D_t^\alpha\vartheta(x,t) = L_1\vartheta(x,t) + L_2\vartheta(x,t) + g(x,t), \tag{6}$$

with initial condition

$$\vartheta(x,0) = c_1(x), \tag{7}$$

where $D_t^\alpha = \dfrac{\partial^\alpha}{\partial t^\alpha}$ presents the Caputo fractional derivative, and L_1 and L_2 express the linear and nonlinear parameters, accordingly, whereas $g(x,t)$ shows the source element.

Thus, $\mathbb{A}$T for Equation (6) yields

$$\mathbb{A}\Big[D_t^\alpha\vartheta(x,t)\Big] = \mathbb{A}\Big[L_1\vartheta(x,t) + L_2\vartheta(x,t) + g(x,t)\Big]. \tag{8}$$

Using the proposition (4) of $\mathbb{A}$T, we obtain

$$h^\alpha\mathbb{A}[\vartheta(x,t)] - \frac{\vartheta(x,0)}{h^{2-\alpha}} = \mathbb{A}\Big[L_1\vartheta(x,t) + L_2\vartheta(x,t) + g(x,t)\Big].$$

After some simplifications, we obtain

$$\mathbb{A}[\vartheta(x,t)] = \frac{\vartheta(x,0)}{h^2} + \frac{1}{h^\alpha}\mathbb{A}\left[L_1\vartheta(x,t) + L_2\vartheta(x,t) + g(x,t)\right],$$

using condition (7), it becomes

$$\mathbb{A}[\vartheta(x,t)] = \frac{c_1(x)}{h^2} + \frac{1}{h^\alpha}\mathbb{A}\left[L_1\vartheta(x,t) + L_2\vartheta(x,t) + g(x,t)\right].$$

Now, applying the inverse $\mathbb{A}$T, we obtain the above equation as follows

$$\vartheta(x,t) = G(x,t) + \mathbb{A}^{-1}\left[\frac{1}{h^\alpha}\mathbb{A}\left\{L_1\vartheta(x,t) + L_2\vartheta(x,t)\right\}\right], \tag{9}$$

where

$$G(x,t) = \mathbb{A}^{-1}\left[\frac{c_1(x)}{h^2} + \frac{1}{h^\alpha}\mathbb{A}\left\{g(x,t)\right\}\right].$$

The HPS reads the results in the terms of power series as follows

$$\vartheta(x,t) = \vartheta_0 + p^1\vartheta_1 + p^2\vartheta_2 + \cdots = \sum_{i=0}^{\infty} p^i\vartheta_i, \tag{10}$$

where $p \in [0,1]$ stands for homotopy parameter.

The nonlinear operator $L_2\vartheta(x,t)$ is defined as follows

$$L_2\vartheta(x,t) = H_0 + p^1H_1 + p^2H_2 + \cdots = \sum_{i=0}^{\infty} p^iH_i(\vartheta), \tag{11}$$

where H_n polynomials are derived as

$$H_n(\vartheta_0,\vartheta_1,\cdots,\vartheta_n) = \frac{1}{n!}\frac{\partial^n}{\partial p^n}\left(L_2\left(\sum_{i=0}^{\infty}p^i\vartheta_i\right)\right)_{p=0}. \quad n = 0,1,2,\cdots \tag{12}$$

Substituting Equations (11) and (12) into Equation (10), we obtain

$$\sum_{i=0}^{\infty} p^i\vartheta_i(x,t) = G(x,t) + p\left[\mathbb{A}^{-1}\left\{\frac{1}{h^\alpha}\mathbb{A}\left(L_1\sum_{i=0}^{\infty}p^i\vartheta_i(x,t) + \sum_{i=0}^{\infty}p^iH_n\right)\right\}\right].$$

Now, we equate the similar powers of p to obtain the following series:

$$\begin{aligned}
p^0 &: \vartheta_0(x,t) = G(x,t),\\
p^1 &: \vartheta_1(x,t) = \mathbb{A}^{-1}\left[\frac{1}{h^\alpha}\mathbb{A}\left\{L_1\vartheta_0(x,t) + H_0(\vartheta)\right\}\right],\\
p^2 &: \vartheta_2(x,t) = \mathbb{A}^{-1}\left[\frac{1}{h^\alpha}\mathbb{A}\left\{L_1\vartheta_1(x,t) + H_1(\vartheta)\right\}\right],\\
p^3 &: \vartheta_3(x,t) = \mathbb{A}^{-1}\left[\frac{1}{h^\alpha}\mathbb{A}\left\{L_1\vartheta_2(x,t) + H_2(\vartheta)\right\}\right],\\
&\vdots
\end{aligned}$$

Continuing these iterations, we can summarize it as

$$\vartheta(x,t) = \vartheta_0(x,t) + p^1\vartheta_1(x,t) + p^2\vartheta_2(x,t) + p^3\vartheta_3(x,t) + \cdots. \tag{13}$$

In limiting cases, when $p \to 1$, we can write it as follows:

$$\vartheta(x,t) = \vartheta_0 + \vartheta_1 + \vartheta_2 + \cdots = \sum_{i=0}^{\infty} \vartheta_i, \tag{14}$$

which shows the approximate solution of the fractional differential problem (5).

4. Convergence Analysis

In this section, we plan to provide the convergence analysis of $\mathbb{A}$HPTS. We aim to demonstrate that the obtained results of Equation (14) converge to the problem of Equation (6). Now, the following theorem is very helpful in providing the sufficient condition of the convergence.

Theorem 1. *Consider that P_1 and P_2 are Banach spaces and $Q : P_1 \to P_2$ is a nonlinear mapping such as*

$$\forall r, r^* \in P_1 : \|Q(r) - Q(r^*)\| \leq \lambda\|r - r^*\|. \quad 0 < \lambda < 1$$

The Banach's fixed point theorem states that, if Q involves a unique point which is fixed with η such that $Q(\eta) = \eta$, then, consider that the sequence in Equation (14) is represented as

$$T_n = Q(T_{n-1}), T_{n-1} = \sum_{i=0}^{n-1} T_i, n = 1,2,3,\cdots$$

and considering that $T_0 = r_0 \in R_r(s)$, where $B_h(r) = \{r^\star \in P_1 \mid \|r^\star - r\| < r\}$, we have (i) $T_n \in C_h(r)$ (ii) $\lim_{n\to\infty} T_n = r$.

Proof.

(i) By the property of mathematical induction, let $n = 1$; we have

$$\|T_1 - r\| = \|Q(T_0) - Q(r)\| \leq \lambda\|r_0 - r\|.$$

Assuming $\|T_{n-1} - r\| \leq \lambda^{n+1}\|r_0 - r\|$ as an induction hypothesis, we obtain

$$\|T_n - r\| = \|Q(T_{n-1}) - Q(r)\| \leq \lambda\|T_{n-1} - r\| \leq \lambda^n\|r_0 - r\|,$$

using the definition of $B_h(r)$, we have

$$\|T_n - r\| \leq \lambda^n\|r_0 - r\| \leq \lambda^n h < h \text{ which implies } T_n \in B_h(r).$$

(ii) As $\|T_n - r\| \leq \lambda^n\|r_0 - r\|$ and $\lim_{n\to\infty} \lambda^n = 0$,

$$\lim_{n\to\infty}\|T_n - r\| = 0, \text{ that is, } \lim_{n\to\infty} T_n = r.$$

□

Hence, the stated statement has been proven.

5. Numerical Applications

In this section, we present the performance of a semi-analytical approach using some numerical applications of time-fractional porous media and heat transfer equations. This scheme shows that the differential problems involving fractional order yield a straightforward recurrence relation and the results are obtained in the form of series. We plotted this in 2D and 3D to show the authenticity of this proposed strategy.

5.1. Problem 1

Consider the nonlinear time-fractional porous media problem such as

$$\frac{\partial^\alpha \vartheta}{\partial t^\alpha} = \frac{\partial}{\partial x}\Big(\vartheta \frac{\partial \vartheta}{\partial x}\Big), \tag{15}$$

with the initial condition

$$\vartheta(x,0) = x, \tag{16}$$

Using $\mathbb{A}$T on Equation (15), we obtain

$$\mathbb{A}\left[\frac{\partial^\alpha \vartheta}{\partial t^\alpha}\right] = \mathbb{A}\left[\frac{\partial}{\partial x}\Big(\vartheta \frac{\partial \vartheta}{\partial x}\Big)\right], \tag{17}$$

$$h^\alpha \mathbb{A}[\vartheta(x,t)] - \frac{\vartheta(x,0)}{h^{2-\alpha}} = \mathbb{A}\left[\frac{\partial}{\partial x}\Big(\vartheta \frac{\partial \vartheta}{\partial x}\Big)\right],$$

$$\mathbb{A}[\vartheta(x,t)] = \frac{\vartheta(x,0)}{h^2} + \frac{1}{h^\alpha}\mathbb{A}\left[\frac{\partial}{\partial x}\Big(\vartheta \frac{\partial \vartheta}{\partial x}\Big)\right].$$

Utilizing the inverse $\mathbb{A}$T, we obtain

$$\vartheta(x,t) = \vartheta(x,0) + \mathbb{A}^{-1}\left[\frac{1}{h^\alpha}\mathbb{A}\Big\{\frac{\partial}{\partial x}\Big(\vartheta \frac{\partial \vartheta}{\partial x}\Big)\Big\}\right]. \tag{18}$$

Now, use HPS to derive the He's components

$$\sum_{i=0}^{\infty} p^i \vartheta_i(x,t) = x + \mathbb{A}^{-1}\Big[\frac{1}{h^\alpha}\mathbb{A}\Big\{\frac{\partial}{\partial x}\sum_{i=0}^{\infty} p^i \vartheta_i \frac{\partial \vartheta_i}{\partial x}\Big\}\Big]. \tag{19}$$

Evaluating similar components of p, we obtain

$$\begin{aligned}
p^0 &: \vartheta_0(x,t) = x,\\
p^1 &: \vartheta_1(x,t) = \mathbb{A}^{-1}\left[\frac{1}{h^\alpha}\mathbb{A}\Big\{\frac{\partial}{\partial x}\Big(\vartheta_0 \frac{\partial \vartheta_0}{\partial x}\Big)\Big\}\right] = \frac{t^\alpha}{\Gamma(\alpha+1)},\\
p^2 &: \vartheta_2(x,t) = \mathbb{A}^{-1}\left[\frac{1}{h^\alpha}\mathbb{A}\Big\{\frac{\partial}{\partial x}\Big(\vartheta_0 \frac{\partial \vartheta_1}{\partial x} + \vartheta_1 \frac{\partial \vartheta_0}{\partial x}\Big)\Big\}\right] = 0,\\
p^3 &: \vartheta_3(x,t) = \mathbb{A}^{-1}\left[\frac{1}{h^\alpha}\mathbb{A}\Big\{\frac{\partial}{\partial x}\Big(\vartheta_0 \frac{\partial \vartheta_2}{\partial x} + \vartheta_1 \frac{\partial \vartheta_1}{\partial x} + \vartheta_2 \frac{\partial \vartheta_0}{\partial x}\Big)\Big\}\right] = 0,\\
&\vdots
\end{aligned}$$

Similarly, we can examine approximation series such as

$$\begin{aligned}
\vartheta(x,t) &= \vartheta_0(x,t) + \vartheta_1(x,t) + \vartheta_2(x,t) + \vartheta_3(x,t) + \vartheta_4(x,t) + \cdots,\\
&= x + \frac{t^\alpha}{\Gamma(\alpha+1)}.
\end{aligned} \tag{20}$$

The exact solution at $\alpha = 1$ states

$$\vartheta(x,t) = x + t. \tag{21}$$

We will now discuss the graphical representations of the time-fractional porous media problem. We sketched the 3D results for the graphical behavior of example 1 in various fractional orders. We obtained the series results by utilizing our proposed technique and then we drew four graphical structures in fractional orders of $\alpha = 0.4, 0.6, 0.8$, and 1 with a domain of $-5 \leq x \leq 5$ and $t = 10$, shown in Figure 1. Table 1 also demonstrates the physical behavior of the approximate solution at different fractional order. We illustrate the 2D graphical structure in Figure 2 at $x = 5$ and $t = 0.01$ to analyze that the increase in fractional order from low to high provides an excellent performance. It states that we may adequately describe any surface by following the appropriate physical processes that exist in the fields of engineering and science.

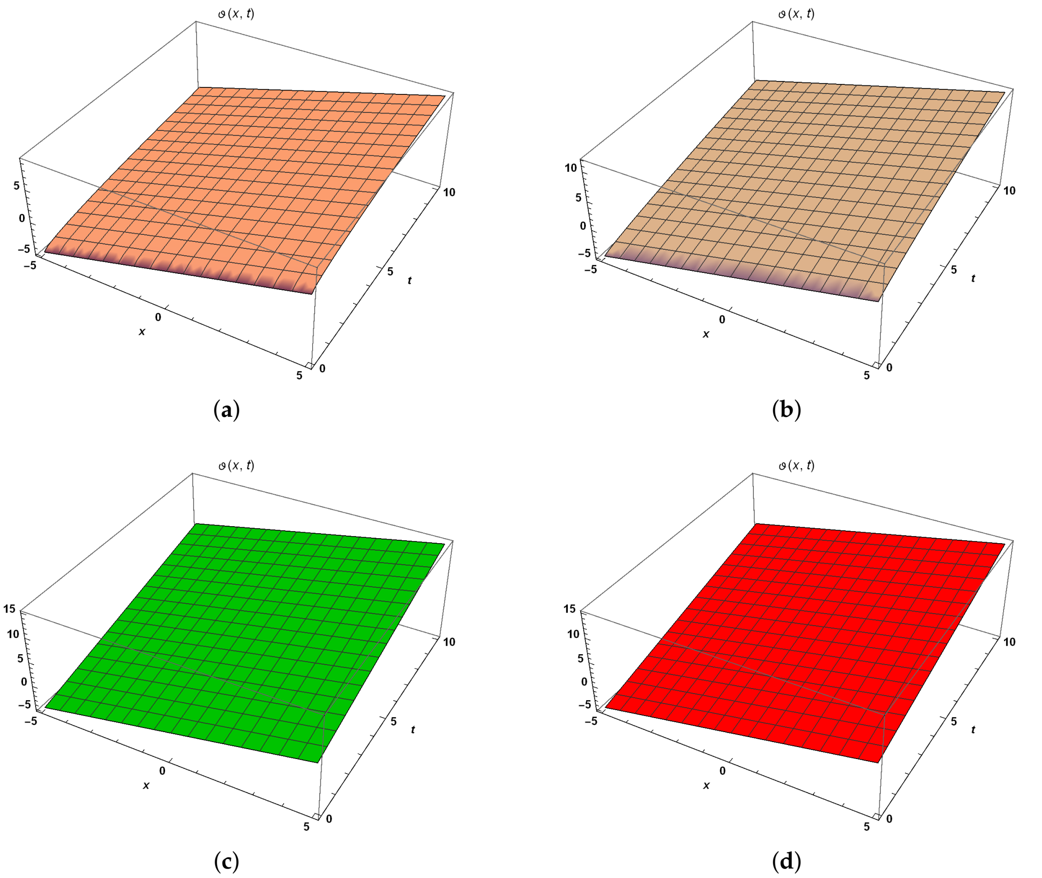

Figure 1. The solution behavior of the approximate solution for $\vartheta_4(x,t)$ at $\alpha = 1$ and the exact solution. (**a**) The approximate solution for Equation (20) at $\alpha = 0.6$. (**b**) The approximate solution for Equation (20) at $\alpha = 0.8$. (**c**) The approximate solution for Equation (20) at $\alpha = 1$. (**d**) The exact solution for Equation (21).

Table 1. The approximate results for distinct parameters of α for example 1.

x	t	$\alpha = 0.25$	$\alpha = 0.50$	$\alpha = 0.75$	$\alpha = 1$
0.1		1.20326	1.22838	1.18807	1.1
0.2		1.30326	1.32838	1.28807	1.2
0.3	1	1.40326	1.42838	1.38807	1.3
0.4		1.50326	1.52838	1.48807	1.4
0.5		1.60326	1.62838	1.58807	1.5
0.1		1.55198	2.05441	2.58025	3.1
0.2		1.65198	2.15441	2.68025	3.2
0.3	3	1.75198	2.25441	2.78025	3.3
0.4		1.85198	2.35441	2.88025	3.4
0.5		1.95198	2.45441	2.98025	3.5
0.1		1.74976	2.62313	3.73817	5.1
0.2		1.84976	2.72313	3.83817	5.2
0.3	5	1.94976	2.82313	3.93817	5.3
0.4		2.04976	2.92313	4.03817	5.4
0.5		2.14976	3.02313	4.13817	5.5

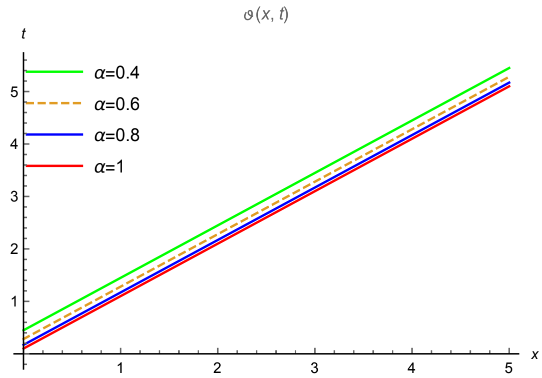

Figure 2. The physical behavior of the approximate solution $\vartheta_4(x,t)$ for $\alpha \in [0.4, 0.6, 0.8, 1]$ compared with the exact solution.

5.2. Problem 2

We consider the nonlinear time-fractional heat transfer problem such as

$$\frac{\partial^\alpha \vartheta}{\partial t^\alpha} = \frac{\partial^2 \vartheta}{\partial x^2} - 2\vartheta^3, \tag{22}$$

with the initial condition

$$\vartheta(x,0) = \frac{1+2x}{x^2+x+1}, \tag{23}$$

Using $\mathbb{A}$T on Equation (13), we obtain

$$\mathbb{A}\left[\frac{\partial^\alpha \vartheta}{\partial t^\alpha}\right] = \mathbb{A}\left[\frac{\partial^2 \vartheta}{\partial x^2} - 2\vartheta^3\right], \tag{24}$$

$$h^{\alpha}\mathbb{A}[\vartheta(x,t)] - \frac{\vartheta(x,0)}{h^{2-\alpha}} = \mathbb{A}\left[\frac{\partial^2\vartheta}{\partial x^2} - 2\vartheta^3\right], \tag{25}$$

$$\mathbb{A}[\vartheta(x,t)] = \frac{\vartheta(x,0)}{h^2} + \frac{1}{h^{\alpha}}\mathbb{A}\left[\frac{\partial^2\vartheta}{\partial x^2} - 2\vartheta^3\right].$$

Utilizing the inverse $\mathbb{A}$T, we obtain

$$\vartheta(x,t) = \vartheta(x,0) + \mathbb{A}^{-1}\left[\frac{1}{h^{\alpha}}\mathbb{A}\left\{\frac{\partial^2\vartheta}{\partial x^2} - 2\vartheta^3\right\}\right]. \tag{26}$$

Now, we use HPS to derive the He's components

$$\sum_{i=0}^{\infty} p^i\vartheta_i(x,t) = x + \mathbb{A}^{-1}\left[\frac{1}{h^{\alpha}}\mathbb{A}\left\{\sum_{i=0}^{\infty} p^i\frac{\partial^2\vartheta_i}{\partial x^2} - 2\sum_{i=0}^{\infty} p^i\vartheta_i^3\right\}\right]. \tag{27}$$

Evaluating similar components of p, we obtain

$$\begin{aligned}
p^0 &: \vartheta_0(x,t) = \frac{1+2x}{x^2+x+1}, \\
p^1 &: \vartheta_1(x,t) = \mathbb{A}^{-1}\left[\frac{1}{h^{\alpha}}\mathbb{A}\left\{\frac{\partial^2\vartheta_0}{\partial x^2} - 2\vartheta_0^3\right\}\right] = \left(\frac{-6(1+2x)}{(1+x+x^2)^2}\right)\frac{t^{\alpha}}{\Gamma(\alpha+1)}, \\
p^2 &: \vartheta_2(x,t) = \mathbb{A}^{-1}\left[\frac{1}{h^{\alpha}}\mathbb{A}\left\{\frac{\partial^2\vartheta_1}{\partial x^2} - 6\vartheta_0^2\vartheta_1\right\}\right] = \left(\frac{72(1+2x)}{(1+x+x^2)^3}\right)\frac{t^{2\alpha}}{\Gamma(2\alpha+1)}, \\
p^3 &: \vartheta_3(x,t) = \mathbb{A}^{-1}\left[\frac{1}{h^{\alpha}}\mathbb{A}\left\{\frac{\partial^2\vartheta_2}{\partial x^2} - 6\vartheta_0\vartheta_1^2 - 6\vartheta_0^2\vartheta_2\right\}\right] = \left(\frac{-1296(1+2x)}{(1+x+x^2)^4} + \frac{216(1+2x)^3}{(1+x+x^2)^5}\right)\frac{t^{3\alpha}}{\Gamma(3\alpha+1)}, \\
&\vdots
\end{aligned}$$

In a similar way, we can consider the approximate series such as

$$\begin{aligned}
\vartheta(x,t) &= \vartheta_0(x,t) + \vartheta_1(x,t) + \vartheta_2(x,t) + \vartheta_3(x,t) + \vartheta_4(x,t) + \cdots, \\
&= \frac{1+2x}{x^2+x+1} - \frac{6(1+2x)}{(1+x+x^2)^2}\frac{t^{\alpha}}{\Gamma(\alpha+1)} + \frac{72(1+2x)}{(1+x+x^2)^3}\frac{t^{2\alpha}}{\Gamma(2\alpha+1)} - \frac{1296(1+2x)}{(1+x+x^2)^4}\frac{t^{3\alpha}}{\Gamma(3\alpha+1)}.
\end{aligned} \tag{28}$$

If $\alpha = 1$, the result is th same as that given by [31,32].

$$\vartheta(x,t) = \frac{1+2x}{x^2+x+1} - \frac{6(1+2x)}{(1+x+x^2)^2}t + \frac{36(1+2x)}{(1+x+x^2)^3}t^2 - \frac{216(1+2x)}{(1+x+x^2)^4}t^3. \tag{29}$$

We will now discuss the graphical representations of the time-fractional heat transfer problem. We sketched the 3D results for the graphical behavior of example 2 in various fractional orders. We obtained the series results by utilizing our proposed technique and then we drew four graphical structures in fractional orders of $\alpha = 0.25, 0.50, 0.75$, and 1 with a domain of $-1 \le x \le 1$ and $t = 1$, shown in Figure 3. Table 2 also demonstrates the physical behavior of the approximate solution at different fractional order. We illustrate the 2D graphical structure in Figure 4 at $x = 5$ and $t = 0.01$ to analyze that the increase in fractional order from low to high provides an excellent performance. It states that we may adequately describe any surface by following the appropriate physical processes that exist in the fields of engineering and science.

Table 2. The approximate results for distinct parameters of α for example 2.

x	t	$\alpha = 0.25$	$\alpha = 0.50$	$\alpha = 0.75$	$\alpha = 1$
0.1		−4.07945	0.911369	1.04676	1.07527
0.2		−2.75201	0.968709	1.09681	1.12321
0.3	0.001	−1.69189	1.00347	1.12166	1.14585
0.4		−0.908809	1.02026	1.12748	1.14943
0.5		−0.358122	1.02333	1.1195	1.13895
0.1		−10.8119	0.782813	1.00654	1.06383
0.2		−7.71798	0.855137	1.05874	1.11288
0.3	0.003	−5.22826	0.904019	1.08662	1.13636
0.4		−3.37602	0.933293	1.09884	1.14068
0.5		−2.06287	0.922491	1.0913	1.13122
0.1		−16.552	0.658231	0.975656	1.05263
0.2		−11.9565	0.753374	1.02932	1.10236
0.3	0.005	−8.24851	0.821376	1.05939	1.12676
0.4		−5.48297	0.865682	1.0711	1.13208
0.5		−3.51699	0.891058	1.06912	1.1236

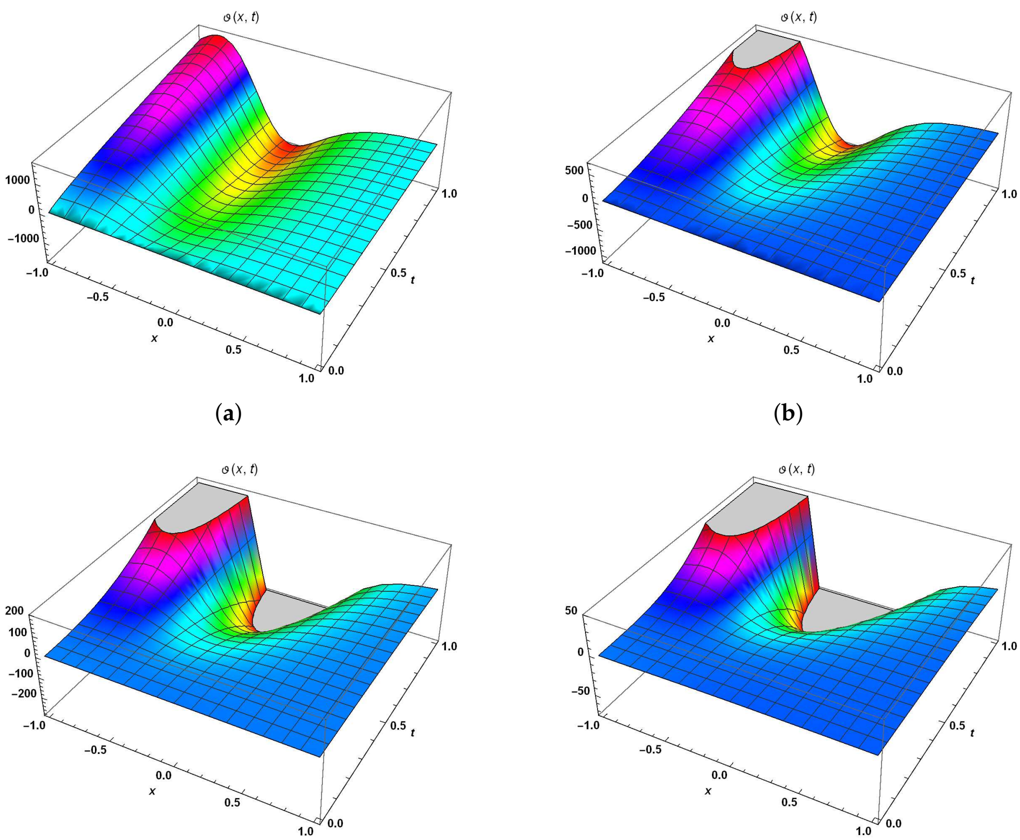

(**a**) (**b**) (**c**) (**d**)

Figure 3. The solution behavior of the approximate solution for $\vartheta_4(x,t)$ at $\alpha = 1$ and the exact solution. (**a**) The approximate solution for Equation (29) at $\alpha = 0.25$. (**b**) The approximate solution for Equation (29) at $\alpha = 0.5$. (**c**) The approximate solution for Equation (29) at $\alpha = 0.75$. (**d**) The approximate solution for Equation (29) at $\alpha = 1$.

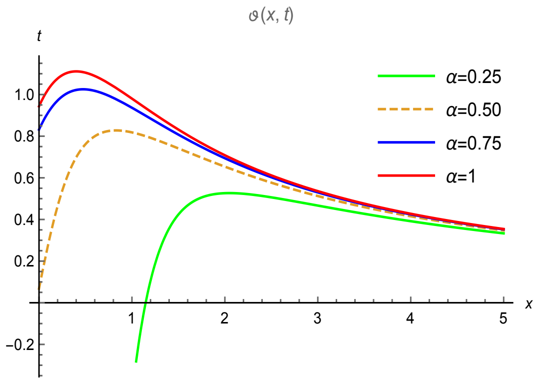

Figure 4. The physical behavior of the approximate solution $\vartheta_4(x,t)$ for $\alpha \in [0.25, 0.5, 0.75, 1]$ compared with the exact solution.

6. Conclusions

In this paper, we successfully obtained the approximate solution of time-fractional porous media and heat transfer equations using a semi-analytical approach. The Abdooh transform converts the fractional problem to a recurrence relation without any perturbation or small parameter of assumption. This recurrence relation is feasible for the process of the homotopy perturbation method to obtain He's polynomials. We observed that these iterations are very easy to compute and converge to the exact solution after a limited series. We demonstrated the 2D and 3D graphical visuals in various fractional order and showed that this proposed scheme has a strong agreement in finding the approximate solution. We considered Mathematica Software 11 to compute the graphical visuals and tabular values. We recommend the audience to study this strategy for the nonlinear fractional-order systems in their future work that exist in the engineering and science fields.

Author Contributions: Investigation, Methodology, Software, and Writing—original draft, M.N.; Writing—review and editing, and supervision, A.I.; Validation and Visualization, S.K.; Conceptualization and Formal analysis, S.M.; Project management and Funding acquisition, L.F.I. All authors have read and consented to submit the article. All authors have read and agreed to the published version of the manuscript.

Funding: This article was supported by the University of Oradea.

Institutional Review Board Statement: Not applicable.

Informed Consent Statement: Not applicable.

Data Availability Statement: Not applicable.

Conflicts of Interest: The authors state that they do not have any competing interests.

References

1. Arrigo, D.J. *Symmetry Analysis of Differential Equations: An Introduction*; John Wiley & Sons: Hoboken, NJ, USA, 2015.
2. Hussain, A.; Bano, S.; Khan, I.; Baleanu, D.; Sooppy Nisar, K. Lie symmetry analysis, explicit solutions and conservation laws of a spatially two-dimensional Burgers–Huxley equation. *Symmetry* **2020**, *12*, 170. [CrossRef]
3. Kumar, S.; Kumar, D. Solitary wave solutions of (3+1)-dimensional extended Zakharov–Kuznetsov equation by Lie symmetry approach. *Comput. Math. Appl.* **2019**, *77*, 2096–2113. [CrossRef]
4. Kumar, S.; Kumar, D.; Kumar, A. Lie symmetry analysis for obtaining the abundant exact solutions, optimal system and dynamics of solitons for a higher-dimensional Fokas equation. *Chaos Solitons Fractals* **2021**, *142*, 110507. [CrossRef]
5. Rashed, A. Analysis of (3+1)-dimensional unsteady gas flow using optimal system of Lie symmetries. *Math. Comput. Simul.* **2019**, *156*, 327–346. [CrossRef]
6. Liu, M.Z.; Cao, X.Q.; Zhu, X.Q.; Liu, B.N.; Peng, K.C. Variational Principles and solitary wave solutions of Generalized Nonliner Schrodinger Equation in the Ocean. *J. Appl. Comput. Mech.* **2021**, *7*, 1639–1648.
7. Song, S.; Chong, D.; Zhao, Q.; Chen, W.; Yan, J. Numerical investigation of the condensation oscillation mechanism of submerged steam jet with high mass flux. *Chem. Eng. Sci.* **2023**, *270*, 118516. [CrossRef]
8. Zhang, J.; Xie, J.; Shi, W.; Huo, Y.; Ren, Z.; He, D. Resonance and bifurcation of fractional quintic Mathieu–Duffing system. *Chaos Interdiscip. J. Nonlinear Sci.* **2023**, *33*, 023131. [CrossRef]

9. Bai, C. Exact solutions for nonlinear partial differential equation: A new approach. *Phys. Lett.* **2001**, *288*, 191–195. [CrossRef]
10. Yavuz, M.; Sulaiman, T.A.; Yusuf, A.; Abdeljawad, T. The Schrödinger-KdV equation of fractional order with Mittag-Leffler nonsingular kernel. *Alex. Eng. J.* **2021**, *60*, 2715–2724. [CrossRef]
11. Hosseini, K.; Akbulut, A.; Baleanu, D.; Salahshour, S. The Sharma–Tasso–Olver–Burgers equation: Its conservation laws and kink solitons. *Commun. Theor. Phys.* **2022**, *74*, 025001. [CrossRef]
12. Ali, K.K.; Abd Elbary, F.; Abdel-wahed, M.S.; Elsisy, M.; Semary, M.S. Solitary Wave Solution for Fractional-Order General Equal-Width Equation via Semi Analytical Technique. *Appl. Math.* **2023**, *17*, 483–493.
13. Khalid, M.Z.; Zubair, M.; Ali, M. An analytical method for the solution of two phase Stefan problem in cylindrical geometry. *Appl. Math. Comput.* **2019**, *342*, 295–308. [CrossRef]
14. Momani, S.; Odibat, Z. Analytical approach to linear fractional partial differential equations arising in fluid mechanics. *Phys. Lett.* **2006**, *355*, 271–279. [CrossRef]
15. Cakmak, M.; Alkan, S. A numerical method for solving a class of systems of nonlinear Pantograph differential equations. *Alex. Eng. J.* **2022**, *61*, 2651–2661. [CrossRef]
16. Nuruddeen, R.; Nass, A.M. Exact solitary wave solution for the fractional and classical GEW-Burgers equations: An application of Kudryashov method. *J. Taibah Univ. Sci.* **2018**, *12*, 309–314. [CrossRef]
17. Iqbal, N.; Botmart, T.; Mohammed, W.W.; Ali, A. Numerical investigation of fractional-order Kersten–Krasil'shchik coupled KdV–mKdV system with Atangana–Baleanu derivative. *Adv. Contin. Discret. Model.* **2022**, *2022*, 1–20. [CrossRef]
18. Mansal, F.; Sene, N. Analysis of fractional fishery model with reserve area in the context of time-fractional order derivative. *Chaos Solitons Fractals* **2020**, *140*, 110200. [CrossRef]
19. Fang, J.; Nadeem, M.; Habib, M.; Karim, S.; Wahash, H.A. A New Iterative Method for the Approximate Solution of Klein-Gordon and Sine-Gordon Equations. *J. Funct. Spaces* **2022**, *2022*. [CrossRef]
20. Shah, K.; Seadawy, A.R.; Arfan, M. Evaluation of one dimensional fuzzy fractional partial differential equations. *Alex. Eng. J.* **2020**, *59*, 3347–3353. [CrossRef]
21. Nadeem, M.; Li, Z. A new strategy for the approximate solution of fourth-order parabolic partial differential equations with fractional derivative. *Int. J. Numer. Methods Heat Fluid Flow* **2022**, *33*, 1062–1075. [CrossRef]
22. Merdan, M. On the solutions of nonlinear fractional Klein–Gordon equation with modified Riemann–Liouville derivative. *Appl. Math. Comput.* **2014**, *242*, 877–888. [CrossRef]
23. Arasteh, H.; Mashayekhi, R.; Toghraie, D.; Karimipour, A.; Bahiraei, M.; Rahbari, A. Optimal arrangements of a heat sink partially filled with multilayered porous media employing hybrid nanofluid. *J. Therm. Anal. Calorim.* **2019**, *137*, 1045–1058. [CrossRef]
24. Barnoon, P.; Toghraie, D.; Dehkordi, R.B.; Afrand, M. Two phase natural convection and thermal radiation of Non-Newtonian nanofluid in a porous cavity considering inclined cavity and size of inside cylinders. *Int. Commun. Heat Mass Transf.* **2019**, *108*, 104285. [CrossRef]
25. Zhao, Y.; Fan, D.; Cao, S.; Lu, W.; Yang, F. Visualization of biochar colloids transport and retention in two-dimensional porous media. *J. Hydrol.* **2023**, *619*, 129266. [CrossRef]
26. Abderrahmane, A.; Jamshed, W.; Abed, A.M.; Smaisim, G.F.; Guedri, K.; Akbari, O.A.; Younis, O.; Baghaei, S. Heat and mass transfer analysis of non-Newtonian power-law nanofluid confined within annulus enclosure using Darcy-Brinkman-Forchheimer model. *Case Stud. Therm. Eng.* **2022**, *40*, 102569. [CrossRef]
27. Sheikholeslami, M.; Shafee, A.; Zareei, A.; Haq, R.u.; Li, Z. Heat transfer of magnetic nanoparticles through porous media including exergy analysis. *J. Mol. Liq.* **2019**, *279*, 719–732. [CrossRef]
28. Seth, G.S.; Bhattacharyya, A.; Kumar, R.; Mishra, M.K. Modeling and numerical simulation of hydromagnetic natural convection Casson fluid flow with nth-order chemical reaction and Newtonian heating in porous medium. *J. Porous Media* **2019**, *22*, 1141–1157 [CrossRef]
29. Aggarwal, S.; Sharma, S.D. Solution of Abel's integral equation by Aboodh transform method. *J. Emerg. Technol. Innov. Res.* **2019**, *6*, 317–325.
30. Aggarwal, S.; Chauhan, R. A comparative study of Mohand and Aboodh transforms. *Int. J. Res. Advent Technol.* **2019**, *7*, 520–529. [CrossRef]
31. Ganji, D.; Sadighi, A. Application of homotopy-perturbation and variational iteration methods to nonlinear heat transfer and porous media equations. *J. Comput. Appl. Math.* **2007**, *207*, 24–34. [CrossRef]
32. Yan, L.M. Modified homotopy perturbation method coupled with Laplace transform for fractional heat transfer and porous media equations. *Therm. Sci.* **2013**, *17*, 1409–1414. [CrossRef]